Biomed Eng Lett (2014) 4:378-387
DOI 10.1007/s13534-014-0149-8

ORIGINAL ARTICLE

Wearable Sensing for Liquid Intake Monitoring *via* Apnea Detection in Breathing Signals

Bo Dong and Subir Biswas

Received: 10 December 2013 / Revised: 13 June 2014 / Accepted: 20 August 2014
© The Korean Society of Medical & Biological Engineering and Springer 2014

Abstract
Purpose Appropriate amount of liquid intake is crucial for maintaining human physiological operations. Traditionally, researchers have used self-reported questionnaires for estimating daily liquid intake, which has been proven to be unreliable. In this study, we developed an instrumented system for liquid intake monitoring to reduce estimation subjectivity by complementing self-reporting information with instrumented data.
Methods Liquid intake can be detected by the way of detecting a person's swallow events. The system works based on a key observation that a person's otherwise continuous breathing process is interrupted by a short apnea when a swallow occurs as a part of the intake process. We detect the swallows *via* recognizing apneas extracted from breathing signal captured by a wearable sensor chest-belt. Such apnea detection is performed using matched filters and machine learning mechanisms with both time and frequency domain features. Spectrum analysis, artifact handling, and iterative template refinement were also proposed, analyzed and experimented with.
Results It is demonstrated that the proposed matched filter method on an average can provide true positive rates up to 82.81% and false positive rates as low as 3.31%. It is also demonstrated that the machine learning method using Decision Tree (J48) provides the best true positive rates up to 97.5% and false positive rates as low as 0.7%.
Conclusions The experiments and analysis suggest that the proposed liquid intake monitoring system and algorithms through breathing signal shows potential for being used for liquid intake monitoring.

Bo Dong (✉), Subir Biswas
Dept. of Electrical and Computer Engineering, Michigan State University, East Lansing, Michigan, US
Tel : +1-517-355-7453 / Fax : +1-517-353-1980
E-mail : dongbo@egr.msu.edu

Keywords Wearable sensing, Swallow detection, Liquid intake monitoring, Breathing pattern analysis, Matched filter

INTRODUCTION

Motivation

Appropriate amount of liquid intake is crucial for maintaining human physiological operations. Prolonged low liquid intake can lead to dehydration and many other undesirable side effects. Dehydration can be a persistent problem for populations such as elderly [1] (especially who live alone) and young athletes undergoing rigorous physical training [2]. It is, therefore, highly desirable to monitor liquid intake as a preventative measure to avoid dehydration and the related problems.

Traditionally, researchers have used self-reported questionnaires for estimating daily liquid intake [3]. In most studies, it is found that self-reporting by elderly population is often unreliable due to their poor memory situations. These make questionnaire-only methods subjective and unreliable [3-5]. An instrumented system for monitoring can reduce subjectivity by complementing such self-reported information with instrumented measurements.

Prior work

Many non-invasive swallow analysis methods are used in the literature. Surface electromyography (SEMG) and sound signal are used in [6] to detect the activation of muscles and the sound of swallow. Fifteen electrodes from the face and throat are used in [7] to record SEMG data during swallowing to analyze dysphagia. The SEMG electrodes are normally attached to the bare skin in the neck region, which raises user acceptability issues due to cosmetic and safety reasons. A two-microphone system is developed in [8] for recording swallow sounds through the ear canal as well as externally

through the air. Placement of such microphones too gives rise to cosmetic issues and therefore its suitability for prolonged practical usage is questionable.

In [9-12], microphones are placed in the neck area near laryngopharynx for detecting the sound of swallowing. Although such methods can provide promising results, it has been shown [13] that placing such equipment on the neck can be uncomfortable and can actually impact the swallowing behavior. Kandori [14] developed a novel magnetic swallow detection system using a magnetic field generating coil and a detection coil installed on a elastic holding structure and placed on two sides of thyroid cartilage. Damouras [15] used a dual axis accelerometer affixed to the thyroid notch for swallow detection in strictly controlled settings. Both of these are not applicable for day to day practical applications.

Piezoelectric sensors are used in [16] to measure the movement of the larynx during swallowing. This method, however, was found to be not very effective for women for whom the larynx movement during swallows is not very prominent. Respiratory Inductance Plethysmography (RIP) is used in [17] for swallow detection by measuring the changes in the cross-sectional area of the rib cage. The RIP belts used for this method are too involving and expensive to be useable for prolonged daily use.

Proposed mechanism

The sensor system and detection algorithms developed in this paper work based on a key observation that a person's otherwise continuous breathing process is interrupted by a short apnea during a swallow, which is a part of the intake process [18]. We first detect swallows by the way of detecting apneas extracted from breathing signal captured by a wearable wireless chest-belt. Afterwards, swallow pattern analysis is used for identifying drinking swallows. Together with self-reporting at the high level of overall liquid intake habits (i.e., the types of drinks etc.), the instrumented detection of liquid swallow counts can offer an objective way to monitor the liquid intake trends.

Key contributions

Contributions of the paper include: 1) proposing a new system level approach towards instrumented swallow detection, 2) developing a number of specific signal processing mechanisms for extracting swallow signatures from breathing signals, and 3) developing an embedded hardware/software platform for implementing and validating the proposed mechanism.

Note that instrumented monitoring for solid food intake can be an equally relevant technology solution. From preliminary experiments we observed different swallow signatures for liquid and solid swallows. In this paper, we focus only on the liquid intake aspects. Results from a general system covering both liquid and solid swallows will be reported in a future publication.

MATERIALS AND METHODS

Sensor system

Fig. 1 shows the developed wearable sensor system belt worn on the chest while collecting and transmitting breathing signal to a PC through a 900 MHz wireless link. The wearable system contains: 1) a piezo-respiratory belt for converting the changes of tension during breathing to a voltage signal, 2) an amplifier and signal shaping circuit for formatting the raw signal to an ADC compatible format, 3) a processor and radio subsystem (Mica2 mote (Crossbow Technology, San Jose, California)) running TinyOS operating system [19], and 4) two *AAAA* batteries. The entire package weighs approximately 20 grams, and the two 600 mAh *AAAA* batteries last for more than 30 hours of continuous operation. We used a piezo-electric respiratory belt for measuring breathing signal, which provides high sensitivity [20] and linearity over a wide range of chest movements. The signal from the belt is sampled by a 10-bit ADC at 30 Hz.

After the signal is received by the 900 MHz access point, it is fed into a PC (processing server) through USB port for detecting swallow events either offline or in real-time. The advantage of using an embedded wireless link is that the developed swallow sensor can be networked with other physiological [21] and physical activity sensors [22] to develop a networked sensing/detection system to provide a complete health monitoring instrumentation package in future.

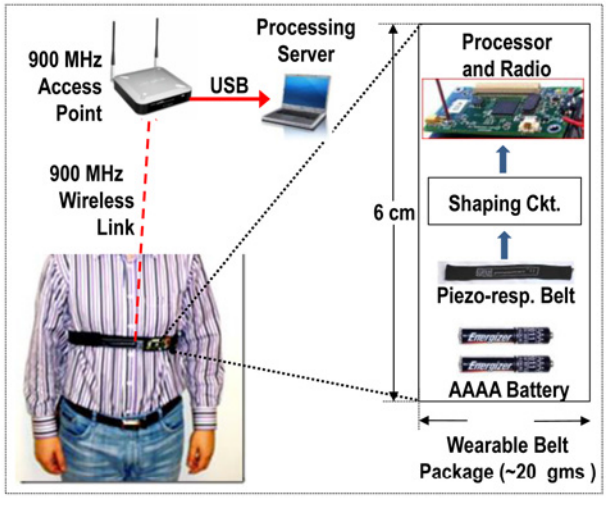

Fig. 1. Wearable wireless food intake monitoring system with a piezo-respiratory chest belt, signal shaping hardware, wireless transceiver, processor, 900MHz wireless link, and a wireless access point connected to a PC for out-of-body processing.

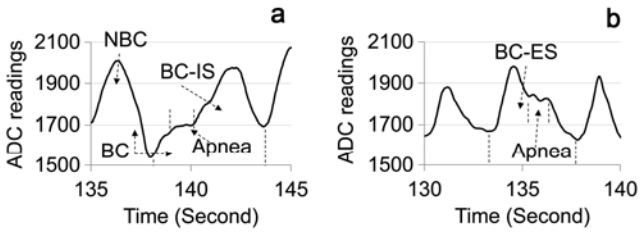

Fig. 2. Examples of *Breathing Cycles* (BC), *Normal Breathing Cycles* (NBC), *Breathing Cycles with Inhale Swallow* (BC-IS), *Breathing Cycles with Exhale Swallow* (BC-ES) and *apnea*.

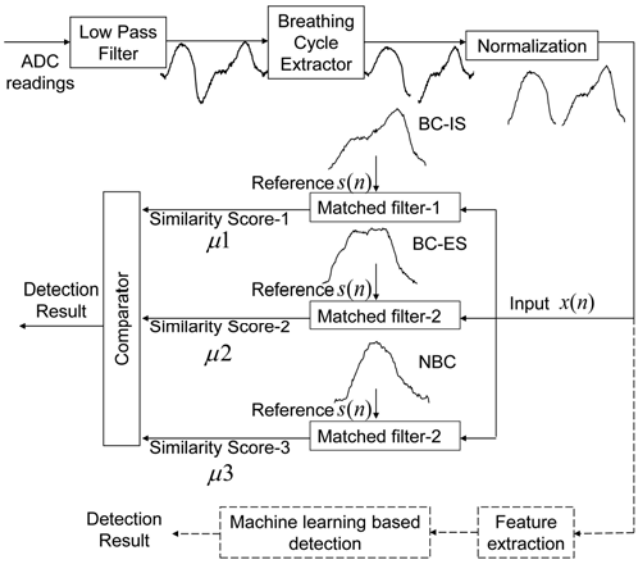

Fig. 3. Apnea signature extraction scheme using matched filter and machine learning methods. The top part shows different stages of signal extraction and shaping before applying the swallow detection methods. The middle and bottom parts show matched filter based and machine learning based methods for swallow detection, respectively.

Breathing, apnea, and swallow signature

Fig. 2 demonstrates two representative human breathing signal segments. The ADC readings in the figure are directly proportional to the elongation of the piezo-electric sensing belt shown in Fig. 1. A breathing cycle can be either normal (i.e., *Normal Breathing Cycle* or *NBC*) or elongated due to a swallow-triggered apnea. A cycle that is elongated due to an apnea at the beginning of an inhale (see Fig. 2a) is termed as *Breathing Cycle with Inhale Swallow* (BC-IS). Fig. 2b shows swallows (i.e., apnea) during the exhale process which are termed as *Breathing Cycles with Exhale Swallow* (BC-ES).

The objective is to be able to classify NBC, BC-ES, and BC-IS with high accuracy. The challenges in detection stem from the fact that there is significant variability in breathing waveforms across different: 1) subjects, 2) measurement instances for the same subject, and most importantly, and 3) the location and duration of the apnea with respect to its breathing cycle.

Matched filter based detection

In what follows we present the performance of a matched filter [23] based template matching mechanism for swallow detection. The template signals for matched filters are chosen from NBCs, BC-ESs, and BC-ISs, so that a breathing cycle can be classified as one of those three by observing the similarity score produced by the respective filters.

As shown in Fig. 3, the signal sampled by ADC at 30Hz is first fed into a low-pass filter for removing any quantization noise. The second step is to extract individual breathing cycles through a peak and valley detector. The next module is for normalizing the extracted cycles in both time and amplitude, so that both input waveform and the reference waveforms of the matched filters [16] have the same amplitude and the number of sample points. Each breathing cycle is normalized to be between 0 and 100 (ADC output units) vertically, and interpolated to 128 sample points. Considering the average length of a breathing cycle of 3.77 seconds in our experiments, the normalized sampling rate after interpolation is approximately 34 Hz. Note that the time-normalization provides a way to handle variable duration breathing cycles and variable duration apnea (i.e., caused by different amount of liquid intake in one swallow) by creating a uniform duration swallow signature. Such a uniform duration signature is then presented to the proposed matched filter and machine learning algorithms.

The normalized breathing cycle waveforms are fed into three separate filters, each with a specific type of reference template waveform. The filters use reference waveforms corresponding to NBC, BC-ES, and BC-IS. The similarity score outputs are compared in order to classify a breathing cycle as one of the above three types of BCs.

Note that the bottom part of Fig. 3 shows how the shaped signal is used for feature extraction and swallow classification of using machine learning based methods.

Machine learning based detection

A machine learning approach with time domain features is applied using all 128 sample points in a normalized breathing cycle. The Toolkit Weka [24] was used for implementing three different classifiers, namely, Support Vector Machine (SVM), Decision Tree (J48), and Naïve Bayes. The classifier parameters are optimized to provide the best accuracy. For SVM, polynomial kernel function is used and the features are normalized. All the other parameters are set to default values. A 10-fold validation approach is used in which the collected breathing cycles are randomly divided into 10 subsets of equal size and a classifier is run for 10 times. In each run, one subset is used for testing while the others are

used for training. 10-fold validation method is used to avoid over-fitting [25].

Breathing signal power at different frequencies, computed using FFT, is also used as features in machine learning. Since FFT is applied on normalized 128-point breathing cycles with a normalized sampling frequency at 34Hz, it produces spectral coefficients for frequencies up to 34 Hz with a granularity of 0.27 Hz. As each normalized breathing cycle is a real finite length series, the resulting 128-point power spectrum are symmetric on $f_s/2$ [26]. Therefore, the first 64 spectral power values are used as the features for driving the classifiers.

Artifact handling

Breathing signal quality often suffers from artifacts including body movements and speech, and liquid intake detection method can be affected by spontaneous swallows [27]. Although anatomically, it is not possible to swallow while talking, people often talk right before or after swallowing. One approach to deal with the talking artifact is to detect talking from the breathing signal itself, and halt the swallow detection process while the talking continues. Fig. 4 demonstrates an example breathing signal segment which contains such speech artifact. Observe that the exhalation parts of the cycles have larger slopes and more undulation, which is caused by modulated air flow through vocal folds while the subject was talking. In this work, we use power spectral density analysis to identify breathing cycles with talking artifacts.

Since upper body movement during food/drink intake is quite common, we conducted experiments with exaggerated upper-torso movement and analyzed the corresponding breathing signal for detecting the movement artifacts.

Spontaneous swallow is a protective aero-digestive reflex for airway protection, and it is caused by accumulated saliva and/or food remnants in the mouth [27]. For healthy subjects, the frequency of spontaneous swallows is about 1.22 times per minute [28]. Due to the fact that the volume of the accumulated saliva and/or food remnants in the mouth is usually small compared to intentional liquid intake, proper parameter training using the matched filter method or machine learning method is able to distinguish liquid swallows from spontaneous swallows. Specifically, we group spontaneous swallows as NBCs during the training phase. This allowed us to differentiate spontaneous swallows from intentional liquid intake with high accuracy.

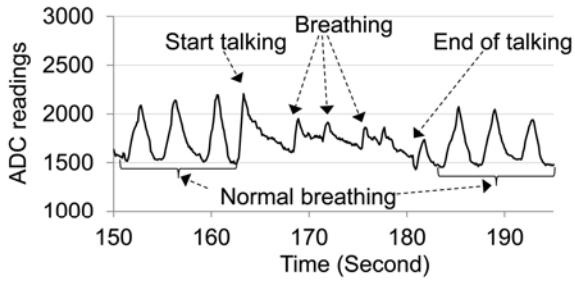

Fig. 4. Breathing signal variability before, during, and after talking.

RESULTS

Experiments using the system in Fig. 1 were carried out with seven subjects (five male and two female) without any known respiratory or swallowing disorders. The belt was worn immediately below to sternum, where the best signal strength was found across all subjects. Each subject performed three sessions, 10 minutes each. In the first 5 minutes, the subject was asked to drink water from a flask with a swallow instruction given once in every 20 seconds. Then the subject conversed with the experimenter for 3 minutes, and in the last 2 minutes, the subject shook their upper body and drank every 20 seconds. Breathing signals from the first 5-minute phase were used for swallow detection, and those from the last 5 minutes were used for artifact handling. The first phase of each session resulted in approximately 80 *Normal Breathing Cycles* (NBCs) and 20 breathing cycles with swallows (both BC-ESs and BC-ISs as shown in Fig. 2). Note that spontaneous swallows (i.e., swallowing saliva) were also included. For the first phase of each session, approximately 100 breathing cycles were recorded in total. For each subject, a *library* containing cycles from three such sessions (i.e., around 300 cycles) was then formed.

The experiments have been approved by Biomedical and Health Institutional Review Board of Michigan State University with IRB number 13-979.

Results for matched filter based detection

Templates or reference waveforms for the matched filters are computed based on cycles from the library as constructed above. A template for NBC is created by sample-by-sample averaging of three randomly chosen NBC breathing cycles from the library. Such randomness adds to the desired variability while forming the template. Similar process is adopted for constructing the templates for BC-IS and BC-ES breathing cycle types. One set of NBC, BC-IS and BC-ES cycles is referred to as a *template combination*.

Fig. 5 shows the performance of matched filter based swallow detection method while using a large number of *template combinations* as the reference signals (i.e., *S(n)*) for all three breathing cycle types. For each subject, 3500 different *template combinations* are first created from the library by choosing different random combinations of NBC, BC-IS and BC-ES cycles while forming the templates. Then, each waveform in the library is classified to be one of NBC,

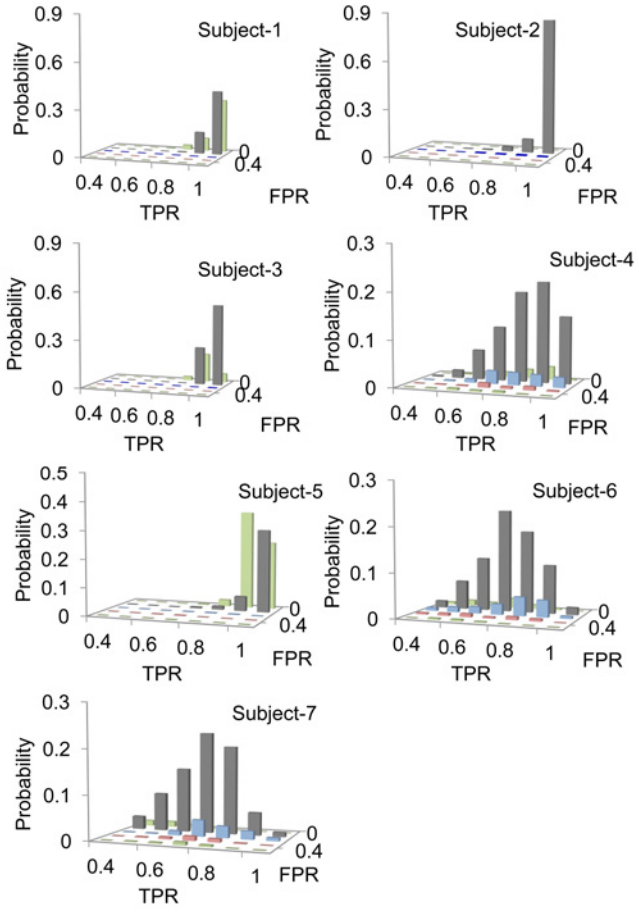

Fig. 5. ROC distribution for all seven subjects with arbitrarily chosen reference templates.

BC-IS or BC-ES using the matched filter-based detection. An ROC pair (*True Positive Rate*, *False Positive Rate*) is finally computed for each of the 3500 *template combinations*. Fig. 5 shows the resulting ROC distributions.

The cluster of high value columns in Fig. 5 indicates that even with arbitrarily chosen template combinations, majority of them offer high *True Positive* and low *False Positive* rates. The spread in the distribution indicates that there exist NBC, BC-IS, and BC-ES waveforms which, if chosen to generate templates, can indeed degrade the system performance. Overall, the true positive rate and false positive rate of all the subjects with all templates are averagely 82.81% and 3.31% respectively.

We experimented with different number of cycles (i.e., three for the above results) for generating the matched filter templates. It was observed that with more cycles, the spread in ROC performance were relatively shorter.

Performance for machine learning based method with time domain features

Classification accuracies for machine learning based methods using time domain features are summarized in Table 1. Results are reported on per-subject basis as well as on combined data from all seven subjects. In the subject specific case, SVM and J48 perform better in terms of both *True* and *False Positive* rates. In the combined case, J48 provides the best swallow detection performance.

Table 1. Performance of classifiers using time domain features.

Subject	Classifier	True Positive Rate±std (%)	False Positive Rate±std (%)
Individual subject	SVM	98.69±2.03	0.14±0.16
	J48	98.8±0.49	0.32±0.14
	Naïve Bayes	97.7±2.62	2.63±2.3
Combined data set	SVM	87.6	1.5
	J48	97.5	0.7
	Naïve Bayes	85.5	9.5

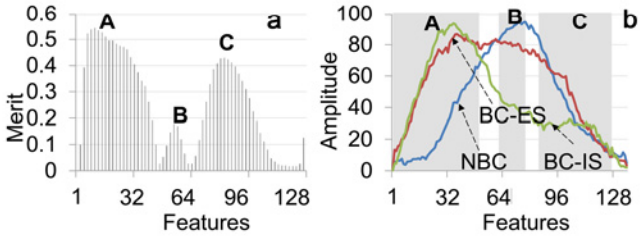

Fig. 6. Utility of the time domain features for Subject-1; three peaks in (a) are caused by different types of breathing cycles with feature distribution shown in (b).

The results of discrimination power analysis of the time-domain features (i.e., all 128 sample points of a breathing cycle) are shown in Fig. 6. Fig. 6a depicts the overall importance of each feature in swallow classification in terms of *merit*. The merit here refers to information gain [29], which is defined as the reduction in class entropy (i.e., $H(*)$) with additional information provided by the feature about the target classes. Assuming A is the feature, C is the set of classes, a and c are instances in A and C respectively, and $p()$ indicates the probability, the following two equations indicate the class entropy before and after providing the feature:

$$H(C) = -\sum_{c \in C} p(c)\log_2 p(c)$$

$$H(C|A) = -\sum_{a \in A} p(a) \sum_{c \in C} p(c|a)\log_2 p(c|a)$$

A feature with higher merit indicates lower class entropy when this feature is adopted. It also indicated higher utility of a feature, which can be used as a guidance factor when feature reduction is needed in the presence of limited computational and storage resources.

There are three distinct utility peaks in Fig. 6a, which can

Table 2. Performance of all three classifiers using frequency domain features. Performance on both individual dataset and the combined dataset are presented in this table.

Subject	Classifier	True Positive Rate±std (%)	False Positive Rate±std (%)
Individual subject	SVM	99.29±1.25	0.09±0.15
	J48	98.8±0.51	0.37±0.17
	Naïve Bayes	95.96±3.03	2.96±1.26
Combined data set	SVM	88.8	2.2
	J48	96.6	0.8
	Naïve Bayes	82.1	4.8

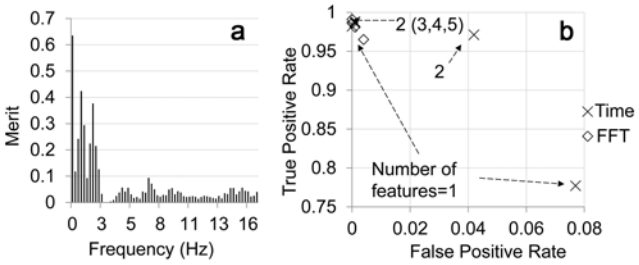

Fig. 7. (a) utility of frequency domain features, (b) comparison between time and frequency domain features; results are presented with limited number of features that are chosen using a method as described.

be explained using the breathing cycles shown in Fig. 6b. The sample points in peak region A are instrumental in distinguishing NBC from BC-IS and BC-ES, and those in region B help distinguishing BC-IS. Finally, the sample points in region C distinguish all three breathing cycle types. The implication of these results is that if a feature reduction is needed, unimportant samples can be eliminated from the areas not in the vicinity of the peaks in Fig. 6a. While the results in Fig. 6a are for subject-1, we have observed very similar patterns of discrimination power for all seven subjects.

Performance for machine learning based method with frequency domain features

Table 2 shows the frequency domain detection performance of 3 classifiers on seven subjects using a 10-fold validation. Similar to the time-domain results, SVM and J48 provides better *True* and *False Positive* rates for subject-specific classification. When classification is done on combined data from all seven subjects, J48 outperforms the other two. Note that in Tables 1 and 2, the standard deviation comes from the variation of true and false positive rates across the subjects. Since for the combined data set scenario in both the tables, the data from all seven subjects are combined into a single data set, standard deviation does not apply to that scenario.

Fig. 7a depicts the overall importance of the spectral power at each frequency. The power in the frequency range 0 (i.e., DC) to approximately 3 Hz contains the most information for differentiating the three target breathing cycle types. Fig. 7b reports the ROC graph with both time and frequency domain features, when only up to 5 features are allowed. The feature sets are selected using the subset evaluation method [29] as follows.

The first feature is selected using the method illustrated in last section which ensures the largest possible reduction in class entropy. The resulting first features are the 10th sample point (out of 128) in time domain, and the DC spectral power in frequency domain. These first features in time and frequency domains can be observed in Fig. 6a and Fig. 7a respectively. Using the same procedure as above, the rest of the four features are added iteratively while maximizing the reduction in class entropy [17].

With more features, the difference in detection performance between the time and frequency domain approaches is negligible. When only one feature is used, however, the frequency domain approach outperforms the time domain approach for the following reason. Fig. 7a demonstrates that the DC component has the highest discriminative power, which can be expressed as:

$$X_{k=0} = \sum_{n=1}^{N-1} x_n e^{-i2\pi\frac{k}{N}n}\Big|_{k=0} = \sum_{n=1}^{N-1} x_n,$$

where $X_{k=0}$ represents the area under curve of the breathing cycle waveform. For BC-ES, since the apnea is located at the beginning of an exhale, its area under curve is much higher than that of NBC and BC-IS. Moreover, majority of the swallows are found to be BC-ES, which is why $X_{k=0}$ alone can be used to achieve considerable detection accuracy. However, no single feature in time domain is able to provide similar discriminative power.

Table 3 summarizes the comparison between the matched filter method and the machine learning method. Observe that machine learning can provide higher detection accuracy compared to the matched filters, although they require a-

Table 3. A comparison between matched filter and machine learning method in liquid intake detection.

	Matched filter method	Machine learning method
Advantages	Smaller training data set required	Higher detection accuracy
Disadvantages	Inferior performance comparing to machine learning method	Larger training data set

priori training. The matched-filters, on the other hand, can achieve acceptable performance using the iterative template refinement algorithm.

It should be noted that both the presented mechanisms are subject-dependent and require personalized training. The subject-dependency stems from the wide diversity of the breathing signals across subjects and their inherently different breathing patterns. In spite of such diversity, however, the swallow signatures were found to be detectable through appropriate algorithm training as proposed for both the techniques.

ADDITIONAL MECHANISMS AND DISCUSSIONS

The performance of matched filter based detection method heavily depends on the selection of reference waveforms. As shown in Fig. 5, improper selection of reference waveform can deteriorate the performance significantly. In what follows we present an iterative template refinement algorithm for incrementally improving the swallow classification performance in a manner that is not very sensitive to the quality of the initially selected templates.

Iterative template refinement

In the first step, an NBC, a BC-IS, and a BC-ES waveform are chosen from the breathing cycle library. Second, all collected breathing cycles are classified using those three waveforms as the templates to the three matched filters. At this stage, each collected cycle is classified as NBC, BC-IS, or BC-ES. Third, all cycles that are classified as NBC are sorted based on their similarity score obtained from the NBC matched filter in the second step. Now, the top 50% of those NBC cycles are sample-by-sample averaged to create the NBC template for the second iteration. The same process is also executed for BC-IS and BC-ES to form the templates for the second iteration. The second and third steps are iteratively repeated till the breathing cycles selected in the third step for generating templates stabilize.

Algorithm 1: Iterative template refinement algorithm

Input: *Initial templates* T_{NBC}, $T_{BC\text{-}IS}$, *and* $T_{BC\text{-}ES}$
while *(templates have not converged)*
  for *(all collected breathing cycle* x_i*)*
    Compute similarity scores $\mu_i^{NBC}, \mu_i^{BC-ES}, \mu_i^{BC-IS}$ *for* x_i
    if $(\mu_i^{NBC} = \max(\mu_i^{NBC}, \mu_i^{BC-ES}, \mu_i^{BC-IS}))$ ***then***
      x_i *is NBC;*
    if $(\mu_i^{BC-ES} = \max(\mu_i^{NBC}, \mu_i^{BC-ES}, \mu_i^{BC-IS}))$ ***then***
      x_i *is BC-ES;*
    if $(\mu_i^{BC-IS} = \max(\mu_i^{NBC}, \mu_i^{BC-ES}, \mu_i^{BC-IS}))$ ***then***
      x_i *is BC-IS;*
  Generate a new set of templates as:
  T_{NBC} = *average (detected NBCs with top 50%* μ_i^{NBC} *)*
  $T_{BC\text{-}ES}$ = *average (detected BC-ESs with top 50%* μ_i^{BC-ES} *)*
  $T_{BC\text{-}IS}$ = *average (detected BC-ISs with top 50%* μ_i^{BC-IS} *)*
return

Stabilization is defined as when the differences between the matched filter similarity scores across consecutive iterations reduce below a pre-defined threshold, which in turn, dictates the overall error performance of the mechanism. The algorithm is summarized in Algorithm 1.

Observe that the overlapping among the three types of breathing cycles is much less in the right graph compared to the left one. This indicates a clear improvement of the matched filter template quality, leading to improved separation of different classified cycle types. The tighter clustering of the points in the right graph provides additional indication to better template quality compared to the starting set. The patterns in Fig. 8 have been consistently observed for a wide

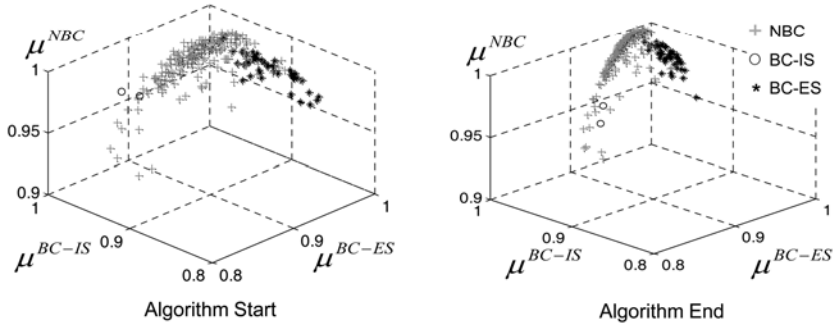

Fig. 8. Similarity score space for: (a) initial matched filter template used as a starting point, and (b) the final template obtained at stabilization of the iterative algorithm. The tighter clustering of the points in the right graph indicates iterative improvement of the template quality.

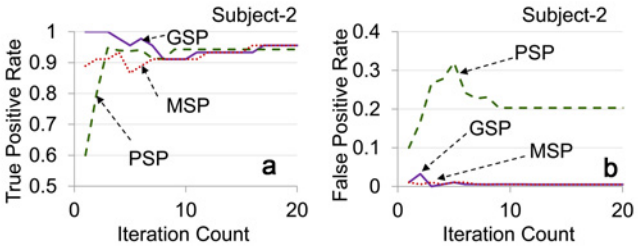

Fig. 9. Iterative template refinement performance; (a) true positive rate, and (b) false positive rate evolution with iterations.

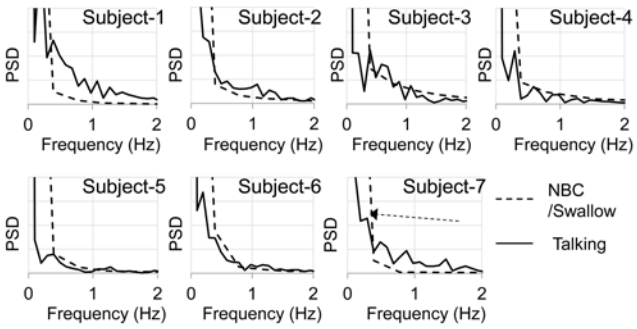

Fig. 10. Power spectral density (PSD) of breathing signals with talking and without talking, when normal breathing or breathing with swallows are executed.

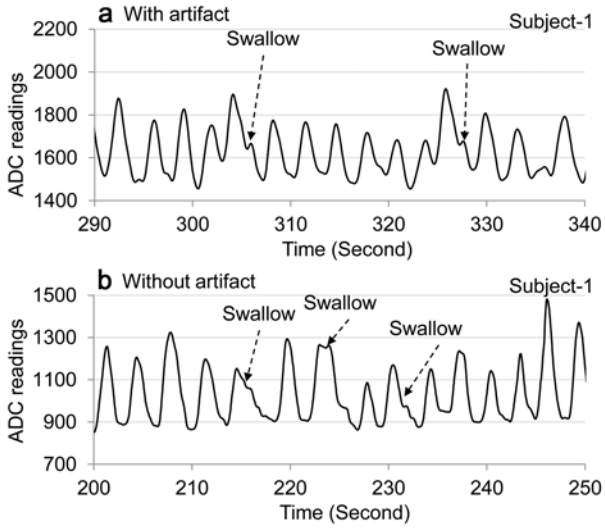

Fig. 11. Breathing signal: (a) with upper body rocking movement, and (b) without movement.

range of initial template quality applied to the data from all seven subjects.

Fig. 9 shows the representative performance of iterative template refinement for a specific subject (i.e., subject-2). The evolution of true and false positive rates are reported for three different starting template sets, termed as, *Good Starting Point* (GSP), *Moderate Starting Point* (MSP), and *Poor Starting Point* (PSP). GSP represents the NBC, BC-IS, and BC-ES combination in the breathing cycle library that provides the highest true positive rate and the lowest false positive rate as evaluated in Fig 5. PSP, on the other hand, represents the combination in the library that provides the lowest true positive rate and the highest false positive rate. Finally, MSP is chosen to be a combination for which the true positive and false positive rates are somewhere in between.

Observe that the true positive rate for PSP consistently improves with iterations. For MSP, such rates either improve or remain constant. With GSP, true positive rates go down slightly, although the decrement is always observed to be much less than the improvements observed for PSP, thus establishing the effectiveness of the approach.

Note that for few PSPs with highly deformed BC-ES or BC-IS waveforms, the false positive rates temporarily go up with iterations before they settle down to lower values. This explains the temporary increase in the false positive rate in Fig. 9b. For the majority of the PSPs, however, the false positive rate remains acceptably low. Results with waveforms from other subjects demonstrated very similar performance patterns.

Artifact handling

We analyzed the undulated exhalation of breathing cycles during talking using power spectral density (PSD). Fig. 10 shows the comparison between PSD of breathing signals during talking (solid lines) and those during NBCs and swallows (dashed lines), while not talking. The density is computed over 4.27-second windows to facilitate 128-point FFT for the 30 Hz sampling rate (4.27 second=128 pts/30 Hz). Observe that the PSDs with talking contain many more variations between 0 and 2 Hz mainly because of the undulations during exhalation as illustrated in Fig. 4. This was consistently observed across a large number of subjects and sessions.

Using the difference in variance between the PSD of received breathing signal and the reference NBC signal, it is possible to identify talking so that the swallow detection process can be halted during talking. Detection of talking is accomplished by using a threshold (of difference in variance), which can be either manually set or can be trained using variance of difference as a feature.

In order to analyze the impacts of upper body movements, in the last 2 minutes of each experimental session, the subject shook their upper body and drank every 20 seconds to simulate changing postures and rocking, which often occurs during drinking. Fig. 11 shows the breathing signals for a subject both with and without such upper torso movements while swallowing.

By comparing the signals with and without artifacts, one can observe that such movement artifacts do not introduce any noticeable changes to the breathing signal, mainly due to the fact that such movement does not change the circumference of the chest area where the belt is placed. Because of this minimal impact, the swallow signatures are well preserved, and can still be clearly discerned using the mechanisms described earlier in the paper. As a result, the proposed mechanism for swallow signature detection does work even when natural upper body movements are present during a swallow process. This observed pattern was consistent across all the other subjects that we have experimented with.

Based on the results, it can be concluded that spontaneous swallows can be accurately detected as NBCs. During each 10-minute session of the experiment, 20 liquid intakes were executed, and according to [28], about 8 spontaneous swallows were present. The overall true positive rate and false positive rate using matched filter method are 82.81% and 3.31% respectively, and 97.5% and 0.7% for machine learning method using time domain features. This high accuracy proves that most of the spontaneous swallows were properly classified.

CONCLUSION AND ONGOING WORK

This paper reported the design, system details, and algorithms for a wearable liquid intake monitoring system. A matched filter based template matching framework, along with a number of template design mechanisms, both static and iterative, were developed for swallow detection with high true positive and low false positive performance. The paper also presented classifier based detection results using both time and frequency domain features. Finally, talking and upper body motion artifacts were analyzed. Ongoing work on the project includes investigating other modalities and methods to detect the volume of liquid consumption, and developing detection algorithms that are capable of handling both solid and liquid swallows.

ACKNOWLEDGEMENT

This project was partially supported by a National Institutes of Health grant R21 HL093395.

CONFLICT OF INTEREST STATEMENTS

Dong B declares that he has no conflict of interest in relation to the work in this article. Biswas S declares that he has no conflict of interest in relation to the work in this article.

REFERENCES

[1] Warren JL, Bacon WE, Harris T, McBean AM, Foley DJ, Phillips C. The burden and outcomes associated with dehydration among US elderly, 1991. Am J Public Health. 1994; 84(8): 1265-9.
[2] Bar-Or O. The young athlete: Some physiological considerations. J Sports Sci. 1995; 13(suppl 1):S31-3.
[3] Vance VA, Woodruff SJ, McCargar LJ, Husted J, Hanning RM. Self-reported dietary energy intake of normal weight, overweight and obese adolescents. Public Health Nutr. 2009; 12(2):222-7.
[4] Schoeller DA. Limitations in the assessment of dietary energy intake by self-report. Metabolism. 1995; 44(2 suppl 2):18-22.
[5] Samuel-Hodge CD, Fernandez LM, Henríquez-Roldán CF, Johnston LF, Keyserling TC. A comparison of self-reported energy intake with total energy expenditure estimated by accelerometer and basal metabolic rate in African-American women with type 2 diabetes. Diabetes Care. 2004; 27(3):663-9.
[6] Amft O, Troster G. Methods for detection and classification of normal swallowing from muscle activation and sound. Conf Proc Pervasive Health Conference and Workshops. 2006; 1-10.
[7] McKeown MJ, Torpey DC, Gehm WC. Non-invasive monitoring of functionally distinct muscle activations during swallowing. Clin Neurophysiol. 2002; 113(3):354-66.
[8] Passler S, Fischer W-J. Food intake activity detection using a wearable microphone system. Conf Proc Intell Environ. 2011; 1:298-301.
[9] Walker WP, Bhatia D. Towards automated ingestion detection: swallow sounds. Conf Proc IEEE Eng Med Biol Soc. 2011; 1:7075-8.
[10] Sazonov E, Schuckers S, Lopez-Meyer P, Makeyev O, Sazonova N, Melanson EL, Neuman M. Non-invasive monitoring of chewing and swallowing for objective quantification of ingestive behavior. Physiol Meas. 2008; 29(5):525-41.
[11] Nagae M, Suzuki K. A neck mounted interface for sensing the swallowing activity based on swallowing sound. Conf Proc IEEE Eng Med Biol Soc. 2011; 1:5224-7.
[12] Makeyev O, Lopez-Meyer P, Schuckers S, Besio W, Sazonov E. Automatic food intake detection based on swallowing sounds. Biomed Signal Process Control. 2012; 7(6):649-56.
[13] Dong B, Biswas S. Swallow monitoring through apnea detection in breathing signal. Conf Proc IEEE Eng Med Biol Soc. 2012; 1:6341-4.
[14] Kandori A, Yamamoto T, Sano Y, Oonuma M, Miyashita T, Murata M, Sakoda S. Simple magnetic swallowing detection system. IEEE Sens J. 2012; 12(4):805-11.
[15] Damouras S, Sejdic E, Steele CM, Chau T. An online swallow detection algorithm based on the quadratic variation of dual-axis accelerometry. IEEE T Signal Process. 2010; 58(6):3352-9.
[16] Danbolt C, Hult P, Grahn LT, Ask P. Validation and characterization of the computerized laryngeal analyzer (CLA) technique. Dysphagia. 1999; 14(4):191-5.
[17] Moreau-Gaudry A, Sabil A, Benchetrit G, Franco A. Use of respiratory inductance plethysmography for the detection of swallowing in the elderly. Dysphagia. 2005; 20(4):297-302.
[18] Dantas RO, Kern MK, Massey BT, Dodds WJ, Kahrilas PJ, Brasseur JG, Cook IJ, Lang IM. Effect of swallowed bolus variables on oral and pharyngeal phases of swallowing. Am J Physiol. 1990; 258(5):G675-81.
[19] TinyOS Home Page. http://www.tinyos.net/. Accessed 12-Sep-2014.
[20] Gautschi G. Piezoelectric Sensorics: Force, Strain, Pressure, Acceleration and Acoustic Emission Sensors, Materials and Amplifiers. 1st ed. New York:Springer; 2002.
[21] Kozlowski SWJ, Chao GT. The dynamics of emergence:

Cognition and cohesion in work teams. Manage Decis Econ. 2012; 33(5-6):335-54.
[22] Dong B, Biswas S. Wearable networked sensing for human mobility and activity analytics: A systems study. Conf Proc Commun Syst Netw. 2012; 1-6.
[23] Turin G. An introduction to matched filters. IRE T Inform Theor. 1960; 6(3):311-29.
[24] Hall M, Frank E, Holmes G, Pfahringer B, Reutemann P, Witten IH. The WEKA data mining software: an update. ACM SIGKDD Explor Newsl. 2009; 11(1):10-8.
[25] Duda RO, Hart PE, Stork DG. Pattern Classification. 2nd ed. New York: Wiley; 2000.
[26] Oppenheim AV, Schafer RW. Discrete-Time Signal Processing 3rd ed. New Jersey: Prentice Hall; 2009.
[27] Crary MA, Carnaby GD, Sia I, Khanna A, Waters MF. Spontaneous swallowing frequency has potential to identify dysphagia in acute stroke. Stroke. 2013; 44(12):3452-7.
[28] Pehlivan M, Yüceyar N, Ertekin C, Çelebi G, Ertaş M, Kalayci T, Aydoğdu I. An electronic device measuring the frequency of spontaneous swallowing: Digital phagometer. Dysphagia. 1996; 11(4):259-64.
[29] Hall MA, Holmes G. Benchmarking attribute selection techniques for discrete class data mining. IEEE T Knowl Data Eng. 2003; 15(6):1437-47.